IAI Journals.ASM.org

Choriodecidual Group B Streptococcal Infection Induces miR-155-5p in the Fetal Lung in *Macaca nemestrina*

Ryan M. McAdams,[a] Craig J. Bierle,[b]* Erica Boldenow,[b] Samantha Weed,[c] Jesse Tsai,[d] Richard P. Beyer,[d] James W. MacDonald,[d] Theo K. Bammler,[d] H. Denny Liggitt,[e] Federico M. Farin,[d] Jeroen Vanderhoeven,[c]* Lakshmi Rajagopal,[b] Kristina M. Adams Waldorf[c]

Department of Pediatrics, University of Washington, Seattle, Washington, USA[a]; Department of Pediatric Infectious Diseases, University of Washington School of Medicine, and Seattle Children's Research Institute, Seattle, Washington, USA[b]; Department of Obstetrics & Gynecology, University of Washington, Seattle, Washington, USA[c]; Department of Environmental and Occupational Health Sciences, University of Washington, Seattle, Washington, USA[d]; Department of Comparative Medicine, University of Washington, Seattle, Washington, USA[e]

The mechanisms underlying fetal lung injury remain poorly defined. MicroRNAs (miRNAs) are small noncoding, endogenous RNAs that regulate gene expression and have been implicated in the pathogenesis of lung disease. Using a nonhuman primate model of choriodecidual infection, we sought to determine if differentially expressed miRNAs were associated with acute fetal lung injury. After inoculating 10 chronically catheterized pregnant monkeys (*Macaca nemestrina*) with either group B streptococcus (GBS) at 1×10^6 CFU ($n = 5$) or saline ($n = 5$) in the choriodecidual space, we extracted fetal lung mRNA and miRNA and profiled the changes in expression by microarray analysis. We identified 9 differentially expressed miRNAs in GBS-exposed fetal lungs, but of these, only miR-155-5p was validated by quantitative reverse transcription-PCR ($P = 0.02$). Significantly elevated miR-155-5p expression was also observed when immortalized human fetal airway epithelial (FeAE) cells were exposed to proinflammatory cytokines (interleukin-6 [IL-6] and tumor necrosis factor alpha [TNF-α]). Overexpression of miR-155-5p in FeAE cells in turn increased the production of IL-6 and CXCL10/gamma interferon-induced protein 10, which are implicated in leukocyte recruitment but also in protection from lung injury. Interestingly, while miR-155-5p decreased fibroblast growth factor 9 (FGF9) expression in a luciferase reporter assay, FGF9 levels were actually increased in GBS-exposed fetal lungs *in vivo*. FGF9 overexpression is associated with abnormal lung development. Thus, upregulation of miR-155-5p may serve as a compensatory mechanism to lessen the increase in FGF9 and prevent aberrant lung development. Understanding the complicated networks regulating lung development in the setting of infection is a key step in identifying how to prevent fetal lung injury leading to bronchopulmonary dysplasia.

The majority of preterm births at less than 28 weeks of gestational age are associated with chorioamnionitis, an inflammation of the fetal membranes due to bacterial infection (1). Chorioamnionitis may contribute to fetal lung injury and increase the risk of development of bronchopulmonary dysplasia (BPD), a type of neonatal chronic lung disease (2). Changes in microRNA (miRNA) expression have previously been associated with BPD in mouse and rat models and have also been known to play important roles in inflammation and immune response pathways (3–5). miRNAs are small noncoding RNAs, 18 to 24 nucleotides in length, that regulate the expression of target genes at the posttranscriptional level by binding to their target mRNAs (6). Similar to protein-coding mRNAs, miRNA expression levels are highly regulated by both transcriptional and posttranscriptional mechanisms (7). The effects of intrauterine infection on fetal lung miRNA expression profiles and the subsequent downstream transcriptional/translational regulatory effects on lung development are unknown. We hypothesized that intrauterine infections affecting the fetal lung may involve differential (miRNA) expression that contributes to early pathways leading to lung injury. The ultimate goal of this study was to discover potential miRNA targets involved in fetal lung injury that could be antagonized to help prevent BPD, for which there are currently no effective therapies.

The group B streptococcus (GBS) is a Gram-positive bacterium that is generally beta-hemolytic and frequently associated with neonatal lung injury (8–10). Our previous studies using a pregnant nonhuman primate model revealed that early choriodecidual GBS infection elevated inflammatory cytokine levels in the amniotic fluid (AF) and induced fetal lung injury (11, 12). Interestingly, despite observations of fetal lung injury and preterm labor (in some cases), bacteria did not translocate into AF or fetal tissues in any of the GBS-infected animals (12). However, differential gene expression was observed in the injured fetal lungs of GBS-infected animals and included the downregulation of pathways involved in angiogenesis and morphogenesis (11). Despite

Received 28 May 2015 **Returned for modification** 27 June 2015
Accepted 13 July 2015

Accepted manuscript posted online 20 July 2015

Citation McAdams RM, Bierle CJ, Boldenow E, Weed S, Tsai J, Beyer RP, MacDonald JW, Bammler TK, Liggitt HD, Farin FM, Vanderhoeven J, Rajagopal L, Adams Waldorf KM. 2015. Choriodecidual group B streptococcal infection induces miR-155-5p in the fetal lung in *Macaca nemestrina*. Infect Immun 83:3909–3917. doi:10.1128/IAI.00695-15.

Editor: A. Camilli

Address correspondence to Lakshmi Rajagopal, lakshmi.rajagopal@seattlechildrens.org, or Kristina M. Adams Waldorf, adamsk@u.washington.edu.

* Present address: Craig J. Bierle, Center for Infectious Diseases and Microbiology Translational Research, University of Minnesota Medical School, Minneapolis, Minnesota, USA; Jeroen Vanderhoeven, Perinatology, Swedish Medical Center, Seattle, Washington, USA.

Supplemental material for this article may be found at http://dx.doi.org/10.1128/IAI.00695-15.

doi:10.1128/IAI.00695-15

these observations, it is unclear if master regulators, such as miRNAs, contribute to the changes in gene expression observed in early fetal lung injury.

In this study, we investigated whether changes in miRNA expression are associated with GBS infection-associated fetal lung injury. Our first aim was to detect differentially expressed miRNAs targeting mRNA genes in the fetal lung in a unique nonhuman primate model. Our second aim was to elucidate potential signaling pathways that induce differential miRNA expression in the fetal lung. Finally, we sought to assess if overexpression of differentially expressed fetal lung miRNA was associated with increased inflammatory cytokine production that may play a role in fetal injury.

MATERIALS AND METHODS

Ethics statement, animals, and study design. This study was carried out in strict accordance with the recommendations in the *Guide for the Care and Use of Laboratory Animals* of the National Research Council (13) and the Weatherall report, *The Use of Non-Human Primates in Research* (14). The protocol was approved by the Institutional Animal Care and Use Committee of the University of Washington (permit number 4165-01). All surgery was performed while the animals were under general anesthesia, and all efforts were made to minimize suffering. A description of the chronically catheterized pregnant nonhuman primate model of chorioamnionitis GBS infection, including details on animal care, analgesia, surgery, fetal euthanasia and necropsy, and fetal lung pathology and scoring, has been previously reported (12, 15). Briefly, 10 chronically catheterized pregnant nonhuman primates (*Macaca nemestrina*) at 118 to 125 days of gestation (term = 172 days) received one of two experimental treatments: (i) choriodecidual and intra-amniotic fluid saline infusions (the saline control group, $n = 5$) or (ii) GBS choriodecidual inoculations (the GBS group; $n = 5$). Both choriodecidual and intra-amniotic fluid saline infusions were used to confirm that neither inoculation was associated with increased AF cytokine levels and were described previously (12). Intra-amniotic fluid pressure was continuously recorded, digitized, and analyzed as reported previously (12). Preterm labor was defined as an intra-amniotic fluid pressure of 10,000 mm Hg · s/h in association with a change in cervical effacement or dilation. The endpoint for the experiments (i.e., cesarean section for tissue collection and delivery by cesarean section for fetal necropsy) was preterm labor or 4 days after GBS inoculation if no preterm labor was observed. AF and fetal blood were collected for cytokine analysis during the course of the experiment, and all fetal organs were harvested at necropsy. Fetal lungs were examined by a board-certified veterinary pathologist who was blinded to the group assignment. Lung histologic sections were evaluated and scored using a semiquantitative scale, as reported previously (12). Components were scored on a scale ranging from 0 to 4 (where 0 is normal) for inflammatory cells, necrosis, and inflammation, including tissue thickening, collapse, or other injury (e.g., fibrin exudation). The lung compartments scored were (i) the vascular/perivascular region, (ii) the bronchial/peribronchial region, and (iii) the alveolar wall, and (iv) the trichrome stain intensity of the lung was also determined. Mononuclear inflammatory cells and neutrophils (which were stained with Leder stain) within alveolar spaces in 5 random ×40 magnification fields were counted. An overall severity score was generated as previously described (12). These data were previously reported (12) and are also shown in Table S1 in the supplemental material.

The preparation of GBS for inoculation into the animals was previously described (12). Briefly, the GBS clinical isolate belonging to the hypervirulent ST-17 clone, capsular serotype III, strain COH-1, was used (16, 17). The COH-1 strain was grown to mid-log phase, and 1×10^6 CFU in phosphate-buffered saline (PBS) was inoculated into the choriodecidual space, as reported previously (12).

RNA extraction from fetal lung tissue and microarray processing. RNA extraction from fetal lung tissue was performed by the Center on Human Development and Disability Genomics Core utilizing the manufacturer's established protocols for the miRNeasy kit (Qiagen, Valencia, CA). RNA quantity and purity were measured with a NanoDrop 8000 spectrophotometer (Thermo Scientific, Waltham, MA), and quality was assessed with an Agilent 2100 bioanalyzer (Agilent Technologies, Santa Clara, CA). Five hundred nanograms of total RNA from each sample was processed for miRNA array analysis. Processing of the RNA samples for the Affymetrix GeneChip miRNA (version 2.0) array was performed according to the standard protocol recommended by the manufacturer (Affymetrix). Hybridized Affymetrix arrays were scanned with an Affymetrix GeneChip 3000 fluorescent scanner. Image generation and feature extraction were performed using Affymetrix GeneChip command console software. The choice of Affymetrix miRNA platform was based on the significant conservation of miRNA species between humans and macaques (18).

miRNA array analysis. Raw microarray data were preprocessed and analyzed with Bioconductor software (http://www.bioconductor.org/) (19). The data were quantile normalized and summarized using the Bioconductor oligonucleotide package. From the normalized data, miRNA transcripts with significant evidence for differential expression were identified using the limma package in Bioconductor. *P* values were calculated with a modified *t* test in conjunction with an empirical Bayes method to moderate the standard errors of the estimated log fold changes. Differentially expressed miRNA transcripts were selected by use of an unadjusted *P* value of <0.05 and an absolute fold change of >1.5.

We excluded one saline control sample from the analysis because this sample was quite different from all other saline samples, as shown in a principal component analysis (see saline sample 3 in Fig. S1 in the supplemental material). We tried using a weighted analysis to account for the differences, but we obtained rather different results when we excluded the sample, which indicates that it had an outsized effect when included in the analysis.

To determine if miRNA expression between the GBS group and the saline group correlated with previously published histopathologic lung severity scores (12), differentially expressed miRNA transcripts were compared to the histopathological lung scores by fitting a two-factor analysis of variance model using the limma package of Bioconductor.

IPA. We used the microRNA target filter feature of the Ingenuity Pathway Analysis (IPA) software (Ingenuity Systems) to determine the predicted mRNA targets of the differentially expressed microRNAs, using the default filter settings. The default settings utilize predicted targets from several databases, including TargetScan, TarBase, miRecords, and Ingenuity Expert Findings. We have previously published mRNA microarray data associated with these experiments, and these are available through Gene Expression Omnibus (GEO) series accession number GSE39029. The microRNA data reported here and the aforementioned mRNA array data were derived from the same samples. We also uploaded our previously published mRNA array data set to the IPA website. This approach allowed us to use IPA's microRNA/mRNA expression pairing function to identify those predicted targets in our mRNA data set that were also differentially expressed (those with a >1.5-fold change in expression between GBS and saline groups with a *P* value of <0.05).

Validation of cDNA microarray by quantitative RT-PCR (qRT-PCR). Reverse transcription (RT) was performed using a TaqMan MicroRNA RT kit (Life Technologies, Carlsbad, CA) following the manufacturer's established protocol for multiplex RT for TaqMan MicroRNA assays. After reverse transcription was completed, real-time PCR was carried out on an ABI Prism 7900 sequence detection system (Life Technologies), and U6 snRNA was used as an endogenous control to normalize microRNA quantitation.

Cells. CCD-1142 human fetal airway epithelial (FeAE) cells (ATCC CRL-2997) were propagated in keratinocyte serum-free medium (Life Technologies) supplemented with 0.05 mg/ml bovine pituitary extract, 5 ng/ml human recombinant epidermal growth factor, and 0.1 mg/ml G-418 (Cellgro). HeLa cells (ATCC CCL-2) were maintained in Dulbecco

modified Eagle medium supplemented with glutamine, 10% fetal bovine serum, and penicillin-streptomycin.

miR-155 expression following cytokine treatment. Confluent CCD-1142 FeAE cells were treated with recombinant human interleukin-1β (IL-1β), IL-6, IL-8, or tumor necrosis factor alpha (TNF-α) at 0.1, 1, 3, 10, and 30 ng/ml. After 24 h, total RNA was isolated from these and untreated cells using a mirVana miRNA isolation kit (Life Technologies) and assessed using a NanoDrop 1000 spectrophotometer (Thermo Scientific). The levels of miR-155 and U6 snRNA were measured by qRT-PCR with TaqMan microRNA assays (assays 002623 and 001973; Applied Biosystems) that were run according to the manufacturer's protocol on an iCycler thermal cycler (Bio-Rad). Each data point represents the average change in miR-155-5p expression observed in three pairs of cytokine-treated samples versus untreated samples. The U6 snRNA expression in each sample was used to normalize for RNA input. qRT-PCRs on each sample were run in duplicate. A Wilcoxon signed-rank test was performed to test for statistical significance.

miR-155 transfection and cytokine analysis. CCD-1142 FeAE cells at 70% confluence were transfected with miRIDIAN hsa-miR-155-5p or negative control 1 (NC1) mimics (catalog numbers C-300647-05 and CN-001000-01, respectively; Thermo Scientific) at the concentrations indicated below using the Lipofectamine RNAiMAX reagent (Life Technologies) according to the manufacturer's protocol. Twenty-four hours later, the tissue culture medium was collected from the cells and cellular debris was pelleted and removed by a 5-min centrifugation at 250 × *g*. The tissue culture medium was subjected to a 30-plex Procarta immunoassay (catalog number PC0015; Affymetrix), and enzyme-linked immunosorbent assays (ELISAs) were used to confirm the expression of C-C chemokine ligand 5 (CCL5), C-X-C motif chemokine 10 (CXCL10), and IL-6 in subsequent experiments (duo sets CCL5-DY278, CXCL10-DY266, and IL-6–DY206, respectively; R&D Systems).

Plasmid construction and luciferase reporter assays. Eukaryotic RNA was purified from CCD-1142 cells using the mirVana miRNA isolation kit and the total RNA isolation protocol (Life Technologies). One microgram of purified RNA was used to synthesize cDNA using SuperScript III reverse transcriptase (Invitrogen, Carlsbad, CA). The 3′ untranslated region (UTR) of the gene for fibroblast growth factor 9 (FGF9) was then amplified using Phusion high-fidelity DNA polymerase (New England BioLabs [NEB], Ipswich, MA) and primers specific for FGF9 (forward primer 5′-CAAAGACAGTTTCTTCACTTGAG-3′, reverse primer 5′-TATGTATTAATGTCTCAAAACTTTTGAC-3′ (Sigma-Aldrich, St. Louis, MO). A PCR product of the expected size (3,066 bp) was purified after agarose gel electrophoresis using a GeneJET PCR purification kit (Thermo Scientific). 3′ A overhangs were added to the PCR product using *Taq* polymerase (NEB), and the PCR product was cloned into the pCR 2.1-TOPO vector according to the manufacturer's protocol (Life Technologies) and transformed via electroporation into ElectroMAX DH5α-E cells following the manufacturer's guidelines (Life Technologies). Insertion of the FGF9 PCR product was confirmed by sequencing (Genewiz, South Plainfield, NJ), and its orientation was confirmed by restriction enzyme digestion. The resulting pCR2.1 plasmid carrying the FGF9 3′ UTR was digested with SacI and XbaI (NEB and Thermo Scientific), and the resulting FGF9 3′ UTR insert was purified using the GeneJET gel extraction kit. The pmirGLO vector was linearized using XbaI (Thermo Scientific) and SacI (NEB) and gel purified according to the protocol supplied with the GeneJET gel extraction kit (Thermo Scientific). The pmirGLO fragment was then ligated with the FGF9 3′ UTR insert using T4 DNA ligase (Thermo Scientific) and transformed via electroporation into ElectroMAX DH5α-E cells following the manufacturer's guidelines (Invitrogen). Restriction enzyme digestion (HindIII [Thermo Scientific], PmeI [NEB], DraIII [NEB], HpaI [NEB]) and DNA sequencing (Genewiz) were used to confirm the presence of the FGF9 3′ UTR in the pmirGLO plasmid.

HeLa cells were seeded at 1.2×10^4 cells per well in 100 μl in a 96-well plate and allowed to reach 90% confluence before transfection. Transfections were performed with the Lipofectamine LTX reagent with the Plus reagent according to the manufacturer's protocol (Life Technologies). One hundred nanograms of plasmid pmirGLO carrying the FGF9 3′ UTR or the pmirGLO control plasmid was used for each well. Transfections were performed in triplicate. In addition to the reporter plasmids, cells were incubated with 100 nM miR-155 or a nonspecific microRNA (Dharmacon, Lafayette, CO) with or without a microRNA inhibitor. Luciferase assays were performed approximately 24 h after transfection using a Dual-Glo luciferase kit (Promega, Fitchburg, WI) per the manufacturer's instruction. Luminescence was measured using a Victor3 multilabel plate reader (PerkinElmer).

TABLE 1 The 9 differentially regulated miRNAs identified by miRNA array[a]

miRNA name	Log_2 fold change	*P* value
hsa-miR-615-3p	0.59	0.002
hsa-miR-769-3p	0.79	0.015
hsa-miR-155-5p	0.70	0.026
hsa-miR-422a	0.64	0.042
hsa-miR-193a-3p	0.94	0.045
hsa-miR-146b-5p	1.70	0.045
hsa-miR-1225-5p	−0.79	0.049
hsa-miR-4324	−0.82	0.011
hsa-miR-514b-5p	−0.60	0.022

[a] The miRNAs were considered differentially up- or downregulated 1.5-fold when the *P* value for changes in expression was <0.05. The prefix "hsa" indicates *Homo sapiens*.

Immunohistochemistry of fetal lung tissues. Immunohistochemistry staining for FGF9 was performed using a rabbit polyclonal FGF9 primary antibody (1:1,000 dilution; catalog number ab71395; Abcam, Cambridge, MA) and a normal rabbit IgG isotype control (1:200 dilution; catalog number I-2000; Vector Laboratories). First, the slides were baked for 30 min at 60°C and deparaffinized on a Leica Bond automated immunostainer (Leica Microsystems, Buffalo Grove, IL). Antigen retrieval was performed by placing the slides in heat-induced epitope retrieval (HIER) citrate buffer for 20 min at 100°C. Blocking consisted of 10% normal goat serum in PBS for 20 min at room temperature. Either the primary antibody (rabbit anti-FGF9) or a rabbit isotype IgG control in Leica primary antibody diluent was applied for 30 min at room temperature. Next, a secondary antibody, goat anti-rabbit immunoglobulin horseradish peroxidase-polymerized secondary antibody (8 μg/ml), was applied for 8 min at room temperature. Antibody complexes were visualized using Leica Bond mixed refine (diaminobenzidine) detection 2 times for 10 min each time at room temperature. Tissues were counterstained with hematoxylin counterstain for 4 min, followed by two rinses in H_2O. Unless otherwise specified, all reagents were obtained from Leica Microsystems.

Microarray data accession number. The miRNA microarray data are available through the GEO database under series accession number GSE60628 (20).

RESULTS

miR-155 is induced in the fetal lung following GBS chorioamnionitis. Our previous studies indicated that early chorioamnionitis GBS infection resulted in fetal lung injury that was associated with the infiltration of inflammatory cells and changes in gene expression in the fetal lung (11, 12). To determine if fetal lung injury was also associated with changes in miRNA expression in the fetal lung following choriodecidual GBS infection, total RNA was isolated from the fetal lung and miRNA expression was measured using human Affymetrix miRNA (version 2.0) microarrays. We observed differential expression (at least 1.5-fold with a *P* value of <0.05; Table 1) in 9 out of 1,100 probe sets (6 were upregulated, 3 were downregulated) in the fetal lung of GBS-infected animals relative to the fetal lung of the saline-treated con-

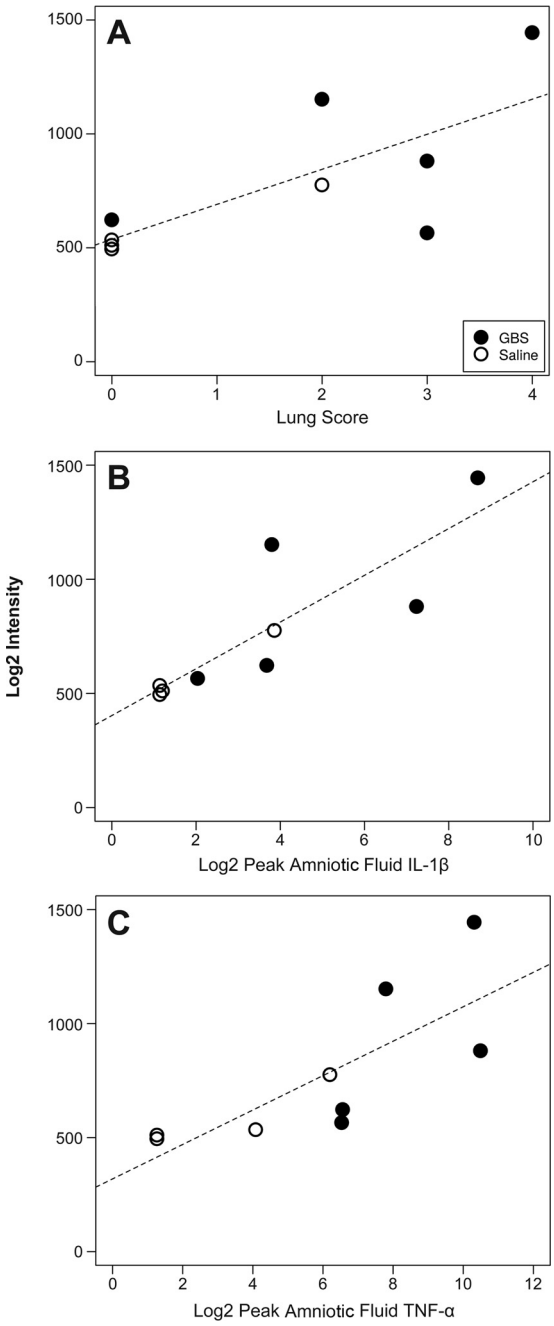

FIG 1 Correlation of fetal lung miR-155-5p expression on the array with fetal histopathologic lung score (A; $R^2 = 0.55$, $P = 0.02$), AF peak IL-1β level (B; $R^2 = 0.71$, $P = 0.004$), and AF peak TNF-α level (C; $R^2 = 0.59$, $P = 0.02$).

trols. Significantly upregulated miRNAs included miR-146b-5p, miR-155-5p, miR-193a-3p, miR-422a, miR-615-3p, and miR-769-3p, whereas miR-1225-5p, miR-4324, and miR-514b-5p were downregulated.

To validate these changes in miRNA expression, we performed qRT-PCR. Of the 9 miRNAs differentially expressed on microarray analysis, only the levels of miR-155-5p were significantly ($P = 0.02$) elevated in the lungs of GBS-exposed fetuses compared with the levels in the controls. The $\log_2$ intensity of miR-155-5p on the array was significantly positively correlated with the fetal lung

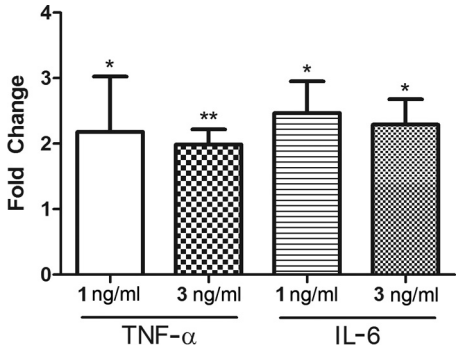

FIG 2 Relative miR-155-5p expression in FeAE cells treated with inflammatory cytokines. The relative expression of miR-155-5p in CCD-1142 FeAE cells treated with IL-6 and TNF-α (1, 3 ng/ml) for 24 h versus that in untreated cells, as measured by qRT-PCR, is shown. Each bar plot represents results from 6 pairs of biological replicates for each data point. Asterisks indicate cytokine treatments where the miR-155-5p levels were significantly different (*, $P < 0.05$; **, $P < 0.015$) by the Wilcoxon signed-rank test. The *y* axis indicates the fold change between cytokine-treated and untreated cells.

score ($R^2 = 0.55$, $P = 0.02$), the AF IL-1β level ($R^2 = 0.71$, $P = 0.004$), and the AF TNF-α level ($R^2 = 0.59$, $P = 0.02$) (Fig. 1). These results illustrate that miR-155-5p expression in the fetal lung is upregulated following choriodecidual GBS exposure and that elevated miR-155-5p levels correlate with fetal lung injury.

miR-155-5p expression is regulated by IL-6 and TNF-α treatment in the airway epithelia. To test our hypothesis that fetal lung exposure to inflammatory cytokines present in AF during a choriodecidual infection could upregulate miR-155-5p, we used a cell line derived from human fetal lungs to model conditions in the fetal lung *in vitro*. We treated CCD-1142 FeAE (E6/E7) cells (21) with a range of concentrations of IL-1β, IL-6, IL-8, and TNF-α (0.1 to 30 ng/ml). After 24 h, total RNA was isolated from these cells, and the levels of miR-155-5p were measured by qRT-PCR. Across multiple experiments, we observed significant increases in miR-155-5p expression relative to that in the untreated controls following treatment with 1 and 3 ng/ml of TNF-α or IL-6 (Fig. 2). The results of these experiments provide support for the hypothesis that the inflammatory cytokines present in the AF following choriodecidual GBS infection may influence the increased expression of miR-155-5p in fetal cells.

miR-155-5p expression in FeAE cells induces CCL5/RANTES, CXCL-10/IP-10, and IL-6 production. Having observed that inflammatory cytokines regulate miR-155-5p expression in FeAE cells, we next sought to determine the biological function of miR-155-5p in this cell type. FeAE cells were transfected with a synthetic miR-155-5p mimic or a scrambled miRNA mimic control. After 24 h, the tissue culture medium was collected from the transfected cells and the levels of cytokines in the medium were measured using either multiplexed immunoassays or ELISAs. We initially screened for changes in the expression of 30 different cytokines following miR-155-5p transfection and found increased levels of IL-6, CCL5/RANTES (also known as regulated upon activation, normal T cell expressed and secreted [RANTES]) and CXCL10 (also known as gamma interferon-induced protein 10 [IP-10]) (data not shown). Subsequent ELISAs confirmed that IL-6, CCL5/RANTES and CXCL10/IP-10 levels in the tissue culture medium were significantly elevated in a dose-dependent manner for cells trans-

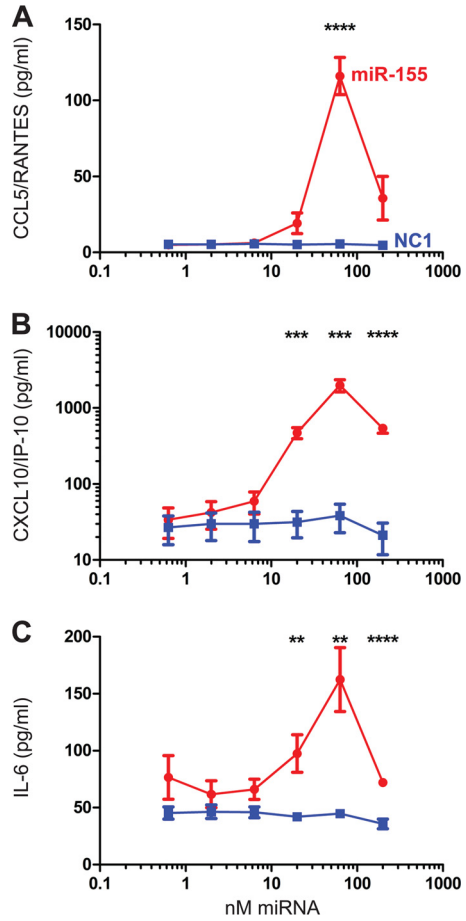

FIG 3 Cytokine production by FeAE cells following miR-155-5p transfection. CCD-1142 FeAE cells were transfected with the indicated concentration of miR-155-5p or a scrambled miRNA control (NC1). After 24 h, the medium was collected from the transfected cells and the levels of CCL5/RANTES (A), CXCL10/IP-10 (B), and IL-6 (C) were measured by ELISA. Asterisks indicate statistically significant differences between miR-155-5p- and scrambled miRNA control-treated cells at a given miRNA concentration (**, $P < 0.05$, ***, $P < 0.01$, ****, $P < 0.0001$) by Student's *t* test. Error bars indicate SEMs.

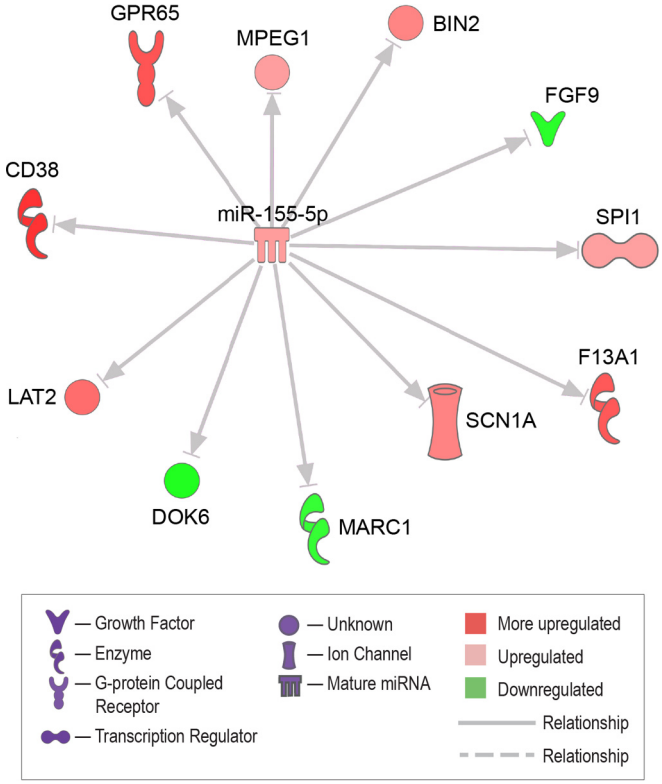

FIG 4 IPA-predicted gene targets of miR-155-5p. The genes shown were filtered for interactions reported in humans only. The color intensity represents the average of the $\log_2$ fold change, with brighter colors representing a more significant difference between the GBS and control groups. Symbols represent the molecular functions described in the key.

fected with miR-155-5p but not in cells transfected with the scrambled miRNA mimic (Fig. 3).

Putative and validated mRNA targets by IPA. We next investigated the putative and validated mRNA targets of miR-155-5p using the IPA microRNA target filter feature to gain insight into the pathogenesis of fetal lung injury or repair (Fig. 4). In a previously published mRNA array study, we identified 335 mRNAs to be differentially expressed in the GBS-treated animals compared to the saline controls (11). When we compared miR-155-5p predicted mRNA targets with the 335 differentially expressed mRNAs, we discovered that they had 11 mRNAs in common, and these are shown in Table 2. These mRNA targets included *BIN2* (bridging integrator 2), *CD38* (cluster of differentiation 38), *DOK6* (docking protein 6; also targeted by miR-193a-3p), *F13A1* (coagulation factor XIII, A1 polypeptide; also targeted by miR-769-3p), *FGF9* (fibroblast growth factor 9), *GPR65* (G protein-coupled receptor 65), *LAT2* (linker for activation of T cells family, member 2), *MARC1* (mitochondrial amidoxime reducing component 1), *MPEG1* (macrophage expressed 1), *SCN1A* (sodium channel, voltage-gated, type 1 alpha subunit; also targeted by miR-193a-3p), and *SPI1* (spleen focus-forming virus proviral integration oncogene). *DOK6*, *FGF9*, and *MARC1* were all downregulated, while the remaining genes were upregulated. *FGF9* is of particular interest, because it was previously shown to influence lung development by regulating mesenchymal growth and induces distal epithelial branching (22).

FGF9 is an mRNA target of miR-155-5p. Bioinformatics analysis using Target Scan indicated that the 3′ UTR of FGF9 contains several predicted miR-155-5p binding sites. We therefore sought

TABLE 2 Intersection of the 11 predicted gene targets of miR-155-5p[a]

Gene symbol	$\log_2$ fold change	*P* value
BIN2	0.89	0.018
CD38	1.47	0.040
DOK6	−0.70	0.001
F13A1	1.20	<0.001
FGF9	−0.66	0.016
GPR65	1.22	0.012
LAT2	1.05	0.034
MARC1[b]	−0.62	0.005
MPEG1	0.69	0.030
SCN1A	0.90	0.032
SPI1[b]	0.68	0.008

[a] The mRNA array genes previously published are described in reference 11.
[b] Genes that have previously been experimentally validated to be targets of miR-155-5p.

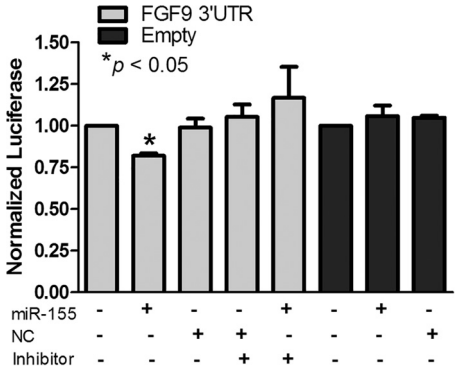

FIG 5 Luciferase reporter assays demonstrating that the FGF9 3′ UTR is an miR-155-5p target. HeLa cells were cotransfected with a luciferase reporter plasmid containing the FGF9 3′ UTR and miR-155-5p or nonspecific (NC) microRNA (100 nM) with or without an miR-155-5p-specific inhibitor. Controls included HeLa cells cotransfected with a control luciferase reporter plasmid and either miR-155-5p or nonspecific microRNA (100 nM). The data represent the mean ± SEM fold change in luciferase activity relative to that for the untreated controls from four independent experiments performed in triplicate.

to verify that FGF9 is a target of miR-155-5p by constructing a luciferase reporter plasmid containing the FGF9 3′ UTR. We observed a significant reduction in luciferase activity ($P < 0.05$) after cotransfection of the luciferase reporter plasmid and miR-155-5p mimics (Fig. 5). In contrast, no change in luciferase activity was observed in cells cotransfected with miR-155-5p and the parental luciferase reporter plasmid that did not include the FGF9 3′ UTR or when nonspecific microRNA was transfected along with the reporter plasmid containing the FGF9 3′ UTR. The addition of an inhibitor specific to miR-155-5p to the cotransfection of the luciferase reporter plasmid and miR-155-5p restored luciferase activity. While the decrease in luciferase expression was modest (<25%), this decrease was not observed in controls and the level of repression was similar to the levels of repression reported for other miRNAs (23). These results indicate that the FGF9 3′ UTR contains an miR-155-5p regulatory element.

Immunohistochemistry for FGF9 expression in fetal lung. Based on the findings presented above, we investigated FGF9 expression in the GBS-infected fetal lungs using immunohistochemistry. Lungs from GBS-infected fetuses displayed a multifocal, widely distributed pattern of alveolar wall staining that intensified in inflammatory foci (Fig. 6). This staining pattern contrasted with that of the lungs from the saline control fetuses, where alveolar wall staining was mildly to minimally present and inflammatory foci were nonexistent.

DISCUSSION

Although some factors are known to be associated with the development of BPD, defining the early biological events in fetal lung injury has remained elusive (24–26). We have identified a single miRNA, miR-155-5p, to be a biomarker of fetal lung injury. miR-155 is an evolutionarily well conserved miRNA that is expressed

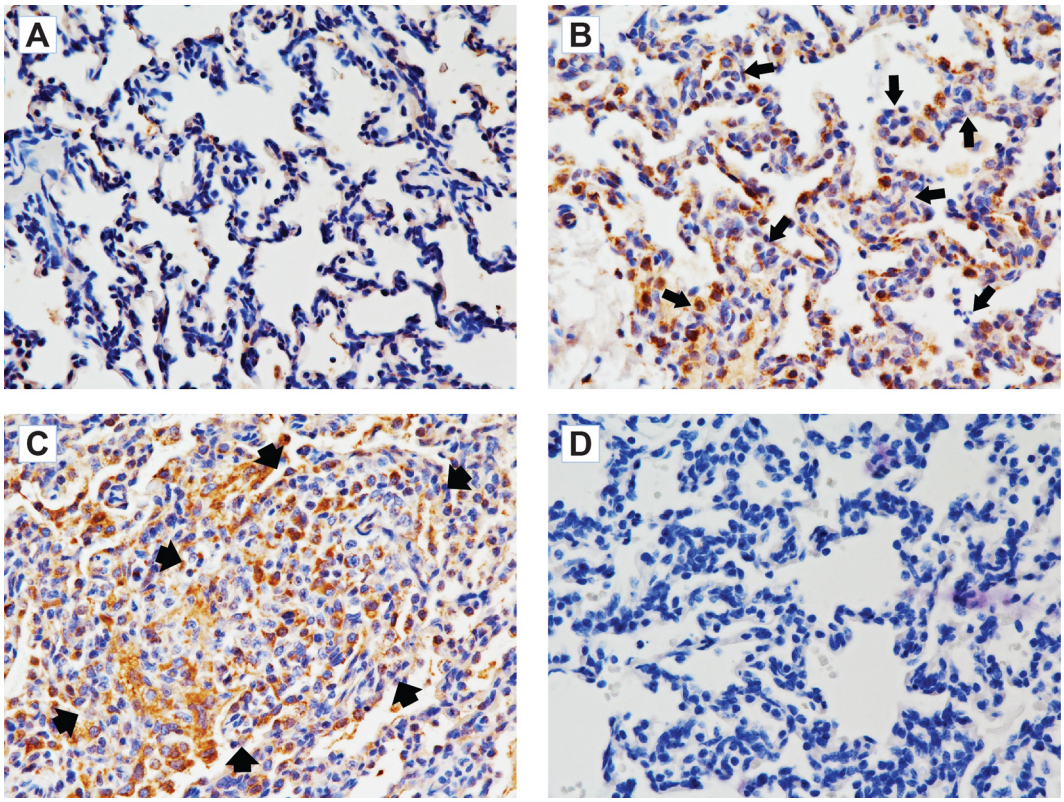

FIG 6 Immunohistochemical staining for FGF9 in the lungs of a saline control fetus (A) and GBS-exposed fetuses (B, C) and in a negative control treated with a rabbit IgG antibody (D). The two panels for different GBS-exposed fetuses are shown to demonstrate FGF9 staining (brown foci) in an area within a dense multicellular inflammatory focus (outlined by arrows in panel C) and in another animal with a less distorted lung architecture but with ample FGF9 staining and scattered inflammatory cells (arrows) associated with focally thickened alveolar walls (B).

primarily in cells of hematopoietic origin and plays a critical role in both innate and adaptive immune responses (7). Proinflammatory mediators (IL-1β, TNF-α, and Toll-like receptors) and monocytes/macrophages can also induce miR-155-5p expression (27, 28). As one of the most well characterized miRNAs, miR-155-5p has more than 140 experimentally validated mRNA targets, including many key regulators of the inflammatory response (i.e., *SHIP1*, *MYD88*, *FADD*, *INPP5D*, *SOCS1*) (7, 29–31). A dual role for miR-155-5p as both an inhibitor and a mediator of inflammation has been described previously and is consistent with our data (7, 30, 31).

Our data suggest that miR-155-5p may have a protective effect on the fetal lung through the induction of CCL5/RANTES and targeting of FGF9. CCL5/RANTES is chemotactic for both monocytes and neutrophils and has a particularly strong effect on neutrophil chemotaxis in the murine lung (32–34) Interestingly, CCL5/RANTES was one of the few proteins associated with a reduced risk of both mild/moderate and severe BPD in infants born prior to 28 weeks of gestation in the ELGAN study (34). CCL5/RANTES has also been shown to have protective effects on organ injury in some animal models (35, 36). Our results also suggest that GBS choriodecidual infection leads to an increase in FGF9 expression in the fetal lungs within 4 days after inoculation. In this context, overexpression of miR-155-5p in the fetal lung may serve as a compensatory mechanism to dampen FGF9 expression to prevent aberrant lung development associated with overexpression (37–39). The upregulation of miR-155 in normal lung human fibroblasts has also been demonstrated to target another member of the fibroblast growth factor family, FGF7, which is involved in early lung organogenesis (40, 41). Like FGF9, the overexpression of FGF7 is associated with aberrant lung development, specifically, development of cystadenomatoid malformations (42). Targeting of the fibroblast growth factor (FGF) pathway (e.g., FGF9 and FGF7 mRNA silencing) by miR-155-5p may be beneficial as a normalizing force on FGF expression. Thus, miR-155-5p may have an important beneficial effect on the developing fetal lung through the induction of CCL5/RANTES and targeting of FGF9 and FGF7.

miR-155-5p may also have a detrimental effect on the fetal lung through the stimulation of IL-6 and CXCL10/IP-10, which are linked to inflammation and other lung diseases (CXCL10/IP-10) (43, 44). While the level of induction of miR-155-5p expression in FeAE cells following treatment with any one cytokine was modest, ranging from 2- to 3-fold, the combined effect of elevated levels of multiple proinflammatory cytokines may contribute to a larger increase *in vivo*. IL-6 is a potent stimulator of monocyte chemotaxis and induces differentiation to macrophages (45). In our model, we have previously reported an increased number of macrophages within the fetal lung interstitium and neutrophils in fetuses exposed to GBS (11). CXCL10/IP-10 is an angiostatic chemokine that is significantly upregulated in the preterm lamb fetal lung following lipopolysaccharide inoculation into the AF; studies report elevated levels of IP-10 in many different lung diseases (44, 46). Other microbes have also been shown to induce miR-155-5p in the fetal/neonatal lung. For example, staphylococcal enterotoxin B exposure (SEB) induced miR-155-5p lung expression in mice, resulting in acute lung injury (47). Interestingly, mice deficient in miR-155-5p had reduced lung inflammation following SEB exposure compared to wild-type animals, suggesting that miR-155-5p was detrimental to the adult lung in a murine model exposed to a different pathogen.

As miR-155-5p is expressed in the fetal lung and has previously been shown to be regulated by cytokines (28), we hypothesize that fetal lung exposure to inflammatory cytokines present in AF during a choriodecidual infection upregulates miR-155-5p. The AF is in direct contact with the fetal lungs due to normal swallowing *in utero*, which has been reported to start to occur at as early as 11 weeks of gestation (48). Although we did not measure AF and fetal lung fluid dynamics, we speculate that AF cytokines migrated to fetal lung fluid based on studies demonstrating bidirectional flow across the trachea in humans under normal conditions and the movement of iron dextran from the intra-amniotic fluid into the fetal lungs with normal fetal breathing (49, 50). Induction of miR-155-5p expression through exposure to AF cytokines could then contribute to a protective or inflammatory response in the pathway of lung injury.

A major strength of the study lies in the many similarities in lung development and immune function between the nonhuman primate and human neonate. The pulmonary morphological and immune features of our nonhuman primate emulate those of humans but differ from those of many other species (51). Both humans and nonhuman primates lack pulmonary intravascular macrophages present in the lungs of many species (e.g., sheep, cattle, pigs), which tend to concentrate toxins and bacteria in the lungs. In contrast, humans and nonhuman primates localize bacteria and toxins in the liver and spleen, which makes their lungs less susceptible to injury than other species (52). There are also many similarities to human pregnancy, including a singleton fetus with a long gestational period, hemomonochorial placentation, and sensitivity to specific pathogens and pathogen-associated molecular patterns (e.g., lipopolysaccharide). Our animal model of infection-associated fetal lung injury also shares similar histopathologic characteristics with BPD, a chronic lung disease characterized by disrupted alveolar development, large airways with inflammation, interstitial fibrosis, and impaired pulmonary angiogenesis (53, 54). The stages of lung development in the nonhuman primate mimic that in the human, which makes it an ideal species to model human fetal lung injury (55).

The main study limitation is our modest sample size, which was necessary for ethical reasons (e.g., conservation of nonhuman primates), as well as the expensive nature of the studies (~$22,000 per animal). Another limitation is that miRNA transfection overexpresses miRNA relative to its natural levels. Interestingly, similar to the findings of our miR-155-5p transfection experiments, we also observed induction of CCL5/RANTES and CXCL10/IP-10 mRNA in the nonhuman primate fetal lung following an *in vivo* GBS infection in a previous study (11). Another limitation, as well as a study strength, is that our results reflect those for an early or limited choriodecidual infection. The gestational timing and the degree and duration of inflammation in our model (which included inflammation resulting from both maternally cleared choriodecidual infections and mild, persistent choriodecidual infections) may have impacted the differential expression of miRNA and mRNA genes. By performing cesarean sections on all animals by 4 days postinfection, we may have interrupted pathways leading to further fetal lung injury, maturation, or repair with additional time *in utero*, which may also affect miRNA expression patterns. The acute histologic changes seen in the GBS-exposed lungs may be precursor findings that subsequently develop into

the histopathologic findings of alveolar simplification and enlargement characteristic of the new BPD after premature infants are exposed to mechanical ventilation, hyperoxia, and/or sepsis (56). Whether a more prolonged and/or increased inflammatory response with bacterial invasion of the AF and fetal lung would further increase the expression of miR-155-5p remains unclear, especially considering the clinical spectrum of lung injury present in preterm neonates born following maternal chorioamnionitis.

In summary, our results suggest that a choriodecidual GBS infection is associated with increased expression of fetal lung miR-155-5p, which is likely to have both beneficial and detrimental effects (11). The ultimate effect of miR-155-5p expression on the fetal lung inflammatory response and FGF expression may be contingent on multiple variables, including the type and virulence of the inciting pathogen, the duration of pathogen/cytokine exposure, the maturity of the lung (the gestational age-dependent response), and the location of the infection/inflammation (e.g., localized versus systemic). Our results add to the complexity of pathways involved in fetal lung injury, which frustrate the efforts to develop therapies aimed at preventing BPD. With no FDA-approved drugs for BPD prevention being currently available, new strategies capable of preventing BPD are needed (57). Future studies are required to determine if the differential expression of miR-155-5p in the fetal lung or the lungs of neonates with risk factors for BPD development may have a beneficial effect and could represent a potential therapy. This approach requires caution, because miR-155-5p expression may also lead to greater IL-6 and IP-10 expression with the propagation of fetal lung injury.

ACKNOWLEDGMENTS

The research reported in this publication was supported by the Eunice Kennedy Shriver National Institute of Child Health and Human Development, the National Institute of Allergy and Infectious Diseases, and the National Center for Research Resources of the National Institutes of Health under award numbers R01AI100989, R56AI070749, R21AI09222, R01AI112619, K08AI067910, K12HD001264, and P30HD002274.

The content is solely the responsibility of the authors and does not necessarily represent the official views of the National Institutes of Health or other funders. The funders had no role in study design, data collection and analysis, decision to publish, or preparation of the manuscript.

We gratefully acknowledge the technical assistance of Jan Hamanishi, Jennifer Summers, and Tony Scauzillo-Golden in preparing the figures. We also acknowledge Craig Rubens and Michael Gravett, who helped to obtain initial grant funding and contributed to the study design related to the performance of the original nonhuman primate experiments.

REFERENCES

1. **Meis PJ, Goldenberg RL, Mercer BM, Iams JD, Moawad AH, Miodovnik M, Menard MK, Caritis SN, Thurnau GR, Dombrowski MP, Das A, Roberts JM, McNellis D.** 2000. Preterm prediction study: is socioeconomic status a risk factor for bacterial vaginosis in black or in white women? Am J Perinatol **17:**41–45. http://dx.doi.org/10.1055/s-2000-7292.
2. **Thomas W, Speer CP.** 2014. Chorioamnionitis is essential in the evolution of bronchopulmonary dysplasia—the case in favour. Paediatr Respir Rev **15:**49–52. http://dx.doi.org/10.1016/j.prrv.2013.09.004.
3. **Eulalio A, Schulte L, Vogel J.** 2012. The mammalian microRNA response to bacterial infections. RNA Biol **9:**742–750. http://dx.doi.org/10.4161/rna.20018.
4. **Baltimore D, Boldin MP, O'Connell RM, Rao DS, Taganov KD.** 2008. MicroRNAs: new regulators of immune cell development and function. Nat Immunol **9:**839–845. http://dx.doi.org/10.1038/ni.f.209.
5. **Yang Y, Qiu J, Kan Q, Zhou XG, Zhou XY.** 2013. MicroRNA expression profiling studies on bronchopulmonary dysplasia: a systematic review and meta-analysis. Genet Mol Res **12:**5195–5206. http://dx.doi.org/10.4238/2013.October.30.4.
6. **Bartel DP.** 2009. MicroRNAs: target recognition and regulatory functions. Cell **136:**215–233. http://dx.doi.org/10.1016/j.cell.2009.01.002.
7. **Elton TS, Selemon H, Elton SM, Parinandi NL.** 2013. Regulation of the MIR155 host gene in physiological and pathological processes. Gene **532:**1–12. http://dx.doi.org/10.1016/j.gene.2012.12.009.
8. **Rubens CE, Raff HV, Jackson JC, Chi EY, Bielitzki JT, Hillier SL.** 1991. Pathophysiology and histopathology of group B streptococcal sepsis in Macaca nemestrina primates induced after intraamniotic inoculation: evidence for bacterial cellular invasion. J Infect Dis **164:**320–330. http://dx.doi.org/10.1093/infdis/164.2.320.
9. **Rubens CE, Smith S, Hulse M, Chi EY, van Belle G.** 1992. Respiratory epithelial cell invasion by group B streptococci. Infect Immun **60:**5157–5163.
10. **Pinnas JL, Strunk RC, Fenton LJ.** 1979. Immunofluorescence in group B streptococcal infection and idiopathic respiratory distress syndrome. Pediatrics **63:**557–561.
11. **McAdams RM, Vanderhoeven J, Beyer RP, Bammler TK, Farin FM, Liggitt HD, Kapur RP, Gravett MG, Rubens CE, Adams Waldorf KM.** 2012. Choriodecidual infection downregulates angiogenesis and morphogenesis pathways in fetal lungs from Macaca nemestrina. PLoS One **7:**e46863. http://dx.doi.org/10.1371/journal.pone.0046863.
12. **Adams Waldorf KM, Gravett MG, McAdams RM, Paolella LJ, Gough GM, Carl DJ, Bansal A, Liggitt HD, Kapur RP, Reitz FB, Rubens CE.** 2011. Choriodecidual group B streptococcal inoculation induces fetal lung injury without intra-amniotic infection and preterm labor in Macaca nemestrina. PLoS One **6:**e28972. http://dx.doi.org/10.1371/journal.pone.0028972.
13. **National Research Council.** 2011. Guide for the care and use of laboratory animals, 8th ed. National Academies Press, Washington, DC.
14. **Weatherall D.** 2006. The use of non-human primates in research. Academy of Medical Sciences, Medical Research Council, The Royal Society, and Wellcome Trust, London, United Kingdom.
15. **Vanderhoeven JP, Bierle CJ, Kapur RP, McAdams RM, Beyer RP, Bammler TK, Farin FM, Bansal A, Spencer M, Deng M, Gravett MG, Rubens CE, Rajagopal L, Adams Waldorf KM.** 2014. Group B streptococcal infection of the choriodecidua induces dysfunction of the cytokeratin network in amniotic epithelium: a pathway to membrane weakening. PLoS Pathog **10:**e1003920. http://dx.doi.org/10.1371/journal.ppat.1003920.
16. **Martin TR, Rubens CE, Wilson CB.** 1988. Lung antibacterial defense mechanisms in infant and adult rats: implications for the pathogenesis of group B streptococcal infections in the neonatal lung. J Infect Dis **157:**91–100. http://dx.doi.org/10.1093/infdis/157.1.91.
17. **Musser JM, Mattingly SJ, Quentin R, Goudeau A, Selander RK.** 1989. Identification of a high-virulence clone of type III Streptococcus agalactiae (group B streptococcus) causing invasive neonatal disease. Proc Natl Acad Sci U S A **86:**4731–4735. http://dx.doi.org/10.1073/pnas.86.12.4731.
18. **Yue J, Sheng Y, Orwig KE.** 2008. Identification of novel homologous microRNA genes in the rhesus macaque genome. BMC Genomics **9:**8. http://dx.doi.org/10.1186/1471-2164-9-8.
19. **Gentleman RC, Carey VJ, Bates DM, Bolstad B, Dettling M, Dudoit S, Ellis B, Gautier L, Ge Y, Gentry J, Hornik K, Hothorn T, Huber W, Iacus S, Irizarry R, Leisch F, Li C, Maechler M, Rossini AJ, Sawitzki G, Smith C, Smyth G, Tierney L, Yang JY, Zhang J.** 2004. Bioconductor: open software development for computational biology and bioinformatics. Genome Biol **5:**R80. http://dx.doi.org/10.1186/gb-2004-5-10-r80.
20. **Barrett T, Wilhite SE, Ledoux P, Evangelista C, Kim IF, Tomashevsky M, Marshall KA, Phillippy KH, Sherman PM, Holko M, Yefanov A, Lee H, Zhang N, Robertson CL, Serova N, Davis S, Soboleva A.** 2013. NCBI GEO: archive for functional genomics data sets—update. Nucleic Acids Res **41:**D991–D995. http://dx.doi.org/10.1093/nar/gks1193.
21. **Lieber M, Smith B, Szakal A, Nelson-Rees W, Todaro G.** 1976. A continuous tumor-cell line from a human lung carcinoma with properties of type II alveolar epithelial cells. Int J Cancer **17:**62–70. http://dx.doi.org/10.1002/ijc.2910170110.
22. **Yin Y, Wang F, Ornitz DM.** 2011. Mesothelial- and epithelial-derived FGF9 have distinct functions in the regulation of lung development. Development **138:**3169–3177. http://dx.doi.org/10.1242/dev.065110.
23. **Zhu S, Si ML, Wu H, Mo YY.** 2007. MicroRNA-21 targets the tumor suppressor gene tropomyosin 1 (TPM1). J Biol Chem **282:**14328–14336. http://dx.doi.org/10.1074/jbc.M611393200.

24. **Yoon BH, Romero R, Kim KS, Park JS, Ki SH, Kim BI, Jun JK.** 1999. A systemic fetal inflammatory response and the development of bronchopulmonary dysplasia. Am J Obstet Gynecol **181:**773–779. http://dx.doi.org/10.1016/S0002-9378(99)70299-1.
25. **Yoon BH, Romero R, Jun JK, Park KH, Park JD, Ghezzi F, Kim BI.** 1997. Amniotic fluid cytokines (interleukin-6, tumor necrosis factor-alpha, interleukin-1 beta, and interleukin-8) and the risk for the development of bronchopulmonary dysplasia. Am J Obstet Gynecol **177:**825–830. http://dx.doi.org/10.1016/S0002-9378(97)70276-X.
26. **Munshi UK, Niu JO, Siddiq MM, Parton LA.** 1997. Elevation of interleukin-8 and interleukin-6 precedes the influx of neutrophils in tracheal aspirates from preterm infants who develop bronchopulmonary dysplasia. Pediatr Pulmonol **24:**331–336. http://dx.doi.org/10.1002/(SICI)1099-0496(199711)24:5<331::AID-PPUL5>3.0.CO;2-L.
27. **Sheedy FJ, O'Neill LA.** 2008. Adding fuel to fire: microRNAs as a new class of mediators of inflammation. Ann Rheum Dis **67**(Suppl 3)**:**iii50–iii55. http://dx.doi.org/10.1136/ard.2008.100289.
28. **O'Connell RM, Taganov KD, Boldin MP, Cheng G, Baltimore D.** 2007. MicroRNA-155 is induced during the macrophage inflammatory response. Proc Natl Acad Sci U S A **104:**1604–1609. http://dx.doi.org/10.1073/pnas.0610731104.
29. **Foster PS, Plank M, Collison A, Tay HL, Kaiko GE, Li J, Johnston SL, Hansbro PM, Kumar RK, Yang M, Mattes J.** 2013. The emerging role of microRNAs in regulating immune and inflammatory responses in the lung. Immunol Rev **253:**198–215. http://dx.doi.org/10.1111/imr.12058.
30. **Sonkoly E, Stahle M, Pivarcsi A.** 2008. MicroRNAs and immunity: novel players in the regulation of normal immune function and inflammation. Semin Cancer Biol **18:**131–140. http://dx.doi.org/10.1016/j.semcancer.2008.01.005.
31. **Staedel C, Darfeuille F.** 2013. MicroRNAs and bacterial infection. Cell Microbiol **15:**1496–1507. http://dx.doi.org/10.1111/cmi.12159.
32. **Schall TJ, Bacon K, Toy KJ, Goeddel DV.** 1990. Selective attraction of monocytes and T lymphocytes of the memory phenotype by cytokine RANTES. Nature **347:**669–671. http://dx.doi.org/10.1038/347669a0.
33. **Pan ZZ, Parkyn L, Ray A, Ray P.** 2000. Inducible lung-specific expression of RANTES: preferential recruitment of neutrophils. Am J Physiol Lung Cell Mol Physiol **279:**L658–L666.
34. **Bose C, Laughon M, Allred EN, Van Marter LJ, O'Shea TM, Ehrenkranz RA, Fichorova R, Leviton A.** 2011. Blood protein concentrations in the first two postnatal weeks that predict bronchopulmonary dysplasia among infants born before the 28th week of gestation. Pediatr Res **69:**347–353. http://dx.doi.org/10.1203/PDR.0b013e31820a58f3.
35. **Shahrara S, Proudfoot AE, Woods JM, Ruth JH, Amin MA, Park CC, Haas CS, Pope RM, Haines GK, Zha YY, Koch AE.** 2005. Amelioration of rat adjuvant-induced arthritis by Met-RANTES. Arthritis Rheum **52:**1907–1919. http://dx.doi.org/10.1002/art.21033.
36. **Dobaczewski M, Xia Y, Bujak M, Gonzalez-Quesada C, Frangogiannis NG.** 2010. CCR5 signaling suppresses inflammation and reduces adverse remodeling of the infarcted heart, mediating recruitment of regulatory T cells. Am J Pathol **176:**2177–2187. http://dx.doi.org/10.2353/ajpath.2010.090759.
37. **Coffey E, Newman DR, Sannes PL.** 2013. Expression of fibroblast growth factor 9 in normal human lung and idiopathic pulmonary fibrosis. J Histochem Cytochem **61:**671–679. http://dx.doi.org/10.1369/0022155413497366.
38. **White AC, Xu J, Yin Y, Smith C, Schmid G, Ornitz DM.** 2006. FGF9 and SHH signaling coordinate lung growth and development through regulation of distinct mesenchymal domains. Development **133:**1507–1517. http://dx.doi.org/10.1242/dev.02313.
39. **Yin Y, White AC, Huh SH, Hilton MJ, Kanazawa H, Long F, Ornitz DM.** 2008. An FGF-WNT gene regulatory network controls lung mesenchyme development. Dev Biol **319:**426–436. http://dx.doi.org/10.1016/j.ydbio.2008.04.009.
40. **Pottier N, Maurin T, Chevalier B, Puissegur MP, Lebrigand K, Robbe-Sermesant K, Bertero T, Lino Cardenas CL, Courcot E, Rios G, Fourre S, Lo-Guidice JM, Marcet B, Cardinaud B, Barbry P, Mari B.** 2009. Identification of keratinocyte growth factor as a target of microRNA-155 in lung fibroblasts: implication in epithelial-mesenchymal interactions. PLoS One **4:**e6718. http://dx.doi.org/10.1371/journal.pone.0006718.
41. **Cardoso WV, Itoh A, Nogawa H, Mason I, Brody JS.** 1997. FGF-1 and FGF-7 induce distinct patterns of growth and differentiation in embryonic lung epithelium. Dev Dyn **208:**398–405. http://dx.doi.org/10.1002/(SICI)1097-0177(199703)208:3<398::AID-AJA10>3.0.CO;2-X.
42. **Tichelaar JW, Lu W, Whitsett JA.** 2000. Conditional expression of fibroblast growth factor-7 in the developing and mature lung. J Biol Chem **275:**11858–11864. http://dx.doi.org/10.1074/jbc.275.16.11858.
43. **Dheda K, Van-Zyl Smit RN, Sechi LA, Badri M, Meldau R, Symons G, Khalfey H, Carr I, Maredza A, Dawson R, Wainright H, Whitelaw A, Bateman ED, Zumla A.** 2009. Clinical diagnostic utility of IP-10 and LAM antigen levels for the diagnosis of tuberculous pleural effusions in a high burden setting. PLoS One **4:**e4689. http://dx.doi.org/10.1371/journal.pone.0004689.
44. **Cannas A, Calvo L, Chiacchio T, Cuzzi G, Vanini V, Lauria FN, Pucci L, Girardi E, Goletti D.** 2010. IP-10 detection in urine is associated with lung diseases. BMC Infect Dis **10:**333. http://dx.doi.org/10.1186/1471-2334-10-333.
45. **Clahsen T, Schaper F.** 2008. Interleukin-6 acts in the fashion of a classical chemokine on monocytic cells by inducing integrin activation, cell adhesion, actin polymerization, chemotaxis, and transmigration. J Leukoc Biol **84:**1521–1529. http://dx.doi.org/10.1189/jlb.0308178.
46. **Kallapur SG, Jobe AH, Ikegami M, Bachurski CJ.** 2003. Increased IP-10 and MIG expression after intra-amniotic endotoxin in preterm lamb lung. Am J Respir Crit Care Med **167:**779–786. http://dx.doi.org/10.1164/rccm.2203030.
47. **Rao R, Nagarkatti P, Nagarkatti M.** 2014. Staphylococcal enterotoxin B-induced microRNA-155 targets SOCS1 to promote acute inflammatory lung injury. Infect Immun **82:**2971–2979. http://dx.doi.org/10.1128/IAI.01666-14.
48. **Diamant NE.** 1985. Development of esophageal function. Am Rev Respir Dis **131:**S29–S32.
49. **Kalache KD, Chaoui R, Bollmann R.** 1997. Doppler assessment of tracheal and nasal fluid flow during fetal breathing movements: preliminary observations. Ultrasound Obstet Gynecol **9:**257–261. http://dx.doi.org/10.1046/j.1469-0705.1997.09040257.x.
50. **Pollack JA, Moise KJ, Jr, Tyson WR, Galan HL.** 2003. The role of fetal breathing motions compared with gasping motions in pulmonary airway uptake of intra-amniotic iron dextran. Am J Obstet Gynecol **189:**958–962. http://dx.doi.org/10.1067/S0002-9378(03)00719-1.
51. **Matute-Bello G, Frevert CW, Martin TR.** 2008. Animal models of acute lung injury. Am J Physiol Lung Cell Mol Physiol **295:**L379–L399. http://dx.doi.org/10.1152/ajplung.00010.2008.
52. **Kallapur SG, Bachurski CJ, Le Cras TD, Joshi SN, Ikegami M, Jobe AH.** 2004. Vascular changes after intra-amniotic endotoxin in preterm lamb lungs. Am J Physiol Lung Cell Mol Physiol **287:**L1178–L1185. http://dx.doi.org/10.1152/ajplung.00049.2004.
53. **Jobe AH.** 2011. The new bronchopulmonary dysplasia. Curr Opin Pediatr **23:**167–172. http://dx.doi.org/10.1097/MOP.0b013e3283423e6b.
54. **Speer CP.** 2003. Inflammation and bronchopulmonary dysplasia. Semin Neonatol **8:**29–38. http://dx.doi.org/10.1016/S1084-2756(02)00190-2.
55. **Yoder BA, Coalson JJ.** 2014. Animal models of bronchopulmonary dysplasia. The preterm baboon models. Am J Physiol Lung Cell Mol Physiol **307:**L970–L977. http://dx.doi.org/10.1152/ajplung.00171.2014.
56. **Coalson JJ.** 2006. Pathology of bronchopulmonary dysplasia. Semin Perinatol **30:**179–184. http://dx.doi.org/10.1053/j.semperi.2006.05.004.
57. **Beam KS, Aliaga S, Ahlfeld SK, Cohen-Wolkowiez M, Smith PB, Laughon MM.** 2014. A systematic review of randomized controlled trials for the prevention of bronchopulmonary dysplasia in infants. J Perinatol **34:**705–710. http://dx.doi.org/10.1038/jp.2014.126.